The Nelson Mandela AFrican Institution of Science and Technology

NM-AIST Repository **https://dspace.mm-aist.ac.tz**

Life sciences and Bio-engineering Research Articles [LISBE]

2023

Conservation of forest biomass and forest–dependent wildlife population: Uncertainty quantification of the model parameters

Fanuel, Ibrahim

Elsevier

https://doi.org/10.1016/j.heliyon.2023.e16948

Provided with love from The Nelson Mandela African Institution of Science and Technology

Heliyon 9 (2023) e16948

Contents lists available at ScienceDirect

Heliyon

journal homepage: www.cell.com/heliyon

Research article

Conservation of forest biomass and forest–dependent wildlife population: Uncertainty quantification of the model parameters

Ibrahim M. Fanuel [a,b,*], Silas Mirau [a], Damian Kajunguri [c], Francis Moyo [d]

[a] Department of Applied Mathematics and Computational Science, Nelson Mandela African Institution of Science and Technology, Arusha, Tanzania
[b] Department of ICT and Mathematics, College of Business Education, Mwanza, Tanzania
[c] Department of Mathematics, Kabale University, Kabale, Uganda
[d] Department of Biodiversity Conservation and Ecosystem Management, Nelson Mandela African Institution of Science and Technology, Arusha, Tanzania

ARTICLE INFO

Keywords:
Uncertainty quantification
Conservation
Forest biomass
Forest–dependent wildlife population
Hypercube Latin sampling

ABSTRACT

The ecosystem is confronted with numerous challenges as a consequence of the escalating human population and its corresponding activities. Among these challenges lies the degradation of forest biomass, which directly contributes to a reduction in forested areas and poses a significant threat to the survival of wildlife species through the intensification of intraspecific competition. In this paper, a non–linear mathematical model to study the conservation of forest and wildlife species that are reliant on forest ecosystem within the framework of human population dynamics and its related activities is developed and analysed. The study assessed the impacts of economic measures in the form of incentives on reducing population pressure on forest resources as well as the potential benefits of technological efforts to accelerate the rate of reforestation. Qualitative and quantitative analyses reveals that economic and technological factors have the potential to contribute to resource conservation efforts. However, these efforts can only be used to a limited extent, and contrary to that, the system will be destabilised. Sensitivity analysis identified the parameters pertaining to human population, human activities, economic measures, and technological efforts as the most influential factors in the model.

1. Introduction

The continuous depletion of forests is a pressing issue that requires attention and scientific investigation [1]. The rapid growth of human population and its associated activities are considered to be the main causes of its depletion [2]. The depletion of forest has a wide range of consequences such as environmental degradation and biodiversity loss [3]. Both human livelihoods and the survival of wildlife species depend on forests. For instance, forests are habitats for 80% – 90% of the terrestrial biodiversity [4], thus, wildlife species are in danger of extinction when forest degradation is uncontrolled. Further, about 1.6 billion people depend entirely or partially on forest resources for their livelihood, making it impossible to completely control access to and utilisation of forest resources [5]. In this situation, sustainable use of forest resources is the only way to ensure that resources are not in risk of extinction while human livelihoods are not jeopardised. To achieve that, information on how forests and human population interacts is very crucial. This information can be obtained in various ways, ranging from theoretical to experimental studies.

* Corresponding author at: Department of Applied Mathematics and Computational Science, Nelson Mandela African Institution of Science and Technology, Arusha, Tanzania.
E-mail address: ibrahimf@nm-aist.ac.tz (I.M. Fanuel).

https://doi.org/10.1016/j.heliyon.2023.e16948
Received 8 March 2023; Received in revised form 31 May 2023; Accepted 1 June 2023

Available online 7 June 2023
2405-8440/© 2023 The Author(s). Published by Elsevier Ltd. This is an open access article under the CC BY-NC-ND license (http://creativecommons.org/licenses/by-nc-nd/4.0/).

In the domain of theoretical studies, which is the focus of this study, various scholars [6–13] used mathematical models to understand the behaviour of system that governs human–forest interaction, the review is available [14]. These models play a crucial role in informing policymakers and facilitating the development of policies and strategies aimed at conserving forest resources. It is important to acknowledge that these models have inherent limitations due to the assumptions made during the modelling process. Nevertheless, their significance lies in their ability to unravel the complexities of the system and provide predictive insights, thereby aiding in understanding and predicting real–world dynamics. However, it is crucial to acknowledge that these models incorporate input parameters that are inherently uncertain due to natural variation and measurement errors [15]. The presence of such uncertainties can affect the accuracy and reliability of the model predictions [15,16]. These uncertainties at the model input propagate through the outputs of the model and complicate the accuracy of the model results. The model output exhibits increased variability as the level of uncertainty in the parameters intensifies [17].

Recently published studies [8,13,18–21] utilised either local sensitivity or single parameter methods to study the uncertainty of input model parameters. These methods typically assume fixed default values for all other parameters, thereby rendering them inadequate for conducting comprehensive uncertainty and sensitivity analysis [15]. Since identification and ultimately control of uncertainties is not guaranteed through the use of single–parameter or local sensitivity analysis methods. In this paper, a non–linear mathematical model aims to study the conservation of forest biomass and wildlife species that rely on forest ecosystem within the framework of human dynamics and its corresponding activities is proposed. The conservation is through the application of economic measures and technological efforts to reduce population pressure and accelerate reforestation. The economic measures can be in the forms of property rights [22], markets and charge systems [23], fiscal instruments [24], and livelihood support [25]. On the other hand, the technological based initiatives can take the form of utilisation of drones and genetically modified seeds [26]. Compared to existing literature on this topic [21,11], the present study integrated the ecological aspects of wildlife species and their dependencies on forest into the model to provide a more holistic understanding of the complex dynamics of human–forest interactions and inform effective forest resource management policies [20]. Additionally, the model considers the saturation of wildlife population, assuming logistic growth which is a more realistic representation of population growth in a limited environment with finite resources to provide insights into long–term sustainability [27].

Furthermore, a multi–dimensional parameter space approach is employed to perform uncertainty and sensitivity analysis of the input parameters. This approach is achieved by combining two statistical methods, namely, the Latin Hypercube Sampling (LHS) and Partial Rank Correlation Coefficient (PRCC) [17]. The LHS method is used to generate random samples in the parameter space, while the PRCC method is used to measure the degree of correlation between the model output and each input parameter. Through the execution of this analysis, we can evaluate the influence of uncertainties in the input parameters on the model predictions and identify the parameters that have the most significant impact. The LHS is a stratified Monte Carlo sampling technique which is effective and offers concurrent sampling of the multi–dimensional parameter space [28], whereby, samples are formed by selecting from equiprobable intervals without replacement [17]. Selection of the method is influenced by its strength to provide an unbiased approximation of the average model output and uses fewer samples to attain the same level of accuracy as other sampling strategies [29,17]. On the other hand, PRCC is a statistical measure that uses rankings rather than values to indicate the degree of linear relationship between a parameter and the model output [30]. It measures the correlation between input parameters and model outputs, while accounting for the presence of other input parameters. The PRCC was selected with the assumptions that the model's parameters are uncertain, and that the parameter and model outputs exhibit both non–linear and monotonic relationships [17]. Furthermore, the PRCC values can be estimated for multiple time steps, providing time–dependent sensitivity analysis instead of a specific time estimates of likely output values [15]. The approach has proven to be among the most robust and efficient sensitivity analysis index methods, the details are available [15,17].

The rest of the paper is organised as follows: The proposed model is shown in Section 2. The model's qualitative and quantitative analyses are presented in Sections 3 and 4, respectively. Section 5 provides the discussion and conclusion.

2. Mathematical model

A non–linear mathematical model (1) is developed to capture the dynamics of variables in a region under consideration. The variables include $B(t)$ representing the density of forest biomass, $W(t)$ representing the density of forest-dependent wildlife population, $N(t)$ representing human population, and $H(t)$ representing human activities at any given time t in the region. The model aims to describe the interplay and changes in these variables over time.

$$\begin{cases} \dot{B} = sB\left(1-\dfrac{B}{L}\right) - \alpha BW - \beta_1 BN - \beta_2 B^2 H + \rho_2 BT_e, \\ \dot{W} = r(B)W\left(1-\dfrac{W}{K(B)}\right) - \nu_1 WN - \nu_2 WH, \\ \dot{N} = \theta N\left(1-\dfrac{N}{M}\right) + \lambda\beta_1 BN - \sigma NW, \\ \dot{P} = \phi N - \phi_0 P - \phi_1 E_f P, \\ \dot{H} = \gamma N + \pi\beta_2 B^2 H + \phi_2 P - \gamma_1 H, \\ \dot{T}_e = \rho(L-B) - \rho_1 T_e, \\ \dot{E}_f = \omega P - \omega_1 E_f, \end{cases} \tag{1}$$

such that,

$$B(0) \geq 0,\ W(0) \geq 0,\ N(0) \geq 0,\ P(0) \geq 0,\ H(0) \geq 0,\ T_e(0) \geq 0,$$

$$E_f(0) \geq 0,\ 0 \leq \lambda \leq 1,\ \leq \pi \leq 1.$$

The first equation of the proposed model captures the logistic growth of forest biomass, with an intrinsic growth rate of s and a carrying capacity of L. The second term represents the predation rate of forest–dependent wildlife species through natural processes, which is modelled using bilinear interaction (αBW) [20]. However, due to the use of forest resources by the human population, forest biomass experiences a reduction in its growth rate, as represented by the term $\beta_1 BN$ [7]. The utilisation of forest resources in the region primarily encompasses activities such as timber harvesting, extraction of medicinal substances, and grazing, among others. Furthermore, forest land is often cleared for agricultural purposes, the construction of housing complexes, and the establishment of industrial infrastructure. As a result, this clearance of forested land diminishes the overall extent of forests within the region, consequently exerting negative impacts on the capacity of forestry resources to sustainably support ecological and human needs. This aspect is explicitly modelled using the fourth term, $\beta_2 B^2 H$ [7], which accounts for the loss of forest land that cannot be used for forest regeneration. The fifth term $\rho_2 BT_e$ expresses the growth of forest biomass after application of technological efforts to restore the cleared forest.

The second equation of the model captures the dynamics of the wildlife population that rely on forest. It follows a logistic growth pattern with a growth rate $r(B)$ and a carrying capacity $K(B)$, both are functions of forest biomass to reflect the species' dependence on the forest ecosystem. The direct depletion of wildlife population by human activities, such as poaching, is modelled using the second term ($\nu_1 WN$) [7]. Meanwhile, the indirect depletion of wildlife caused by human activities, such as habitat destruction or fragmentation, is modelled using the third term ($\nu_2 WH$). The third equation of the model describes the dynamics of the human population, assuming a logistic growth pattern. This growth pattern is characterised by an intrinsic growth rate θ, and a carrying capacity M. The term $\lambda\beta_1 BN$ in the model represents the additional growth of the human population due to the use of forest resources for their livelihood [21]. Furthermore, human population is depleted by interaction with wild animals, for example, in some regions of sub–Saharan Africa, human populations have been threatened by wildlife predators like lions and leopards [31]. This particular aspect is captured in the model through the inclusion of the third term (σNW).

The fourth equation describes the dynamics of population pressure, which increases proportionally to the human population with a growth rate ϕ. Additionally, population pressure is subject to natural depletion ($\phi_0 P$) and depletion through economic measures ($\phi_1 E_f P$) designed to support livelihoods and regulate resource exploitation [21]. The dynamics of human activities in the forest ecosystem are modelled in equations five. It is assumed that human activities grow proportionally to the density of human population (γN) and population pressure ($\phi_2 P$) [20]. Furthermore, the growth of human activities is driven by the benefits obtained from the forest and depletes naturally with depletion rate γ_1.

The implementation of technological efforts to accelerate the rate of reforestation is described in equation six. The rate of technological efforts is postulated to be proportional to the difference between the carrying capacity of the forest and the current level of forest biomass ($\rho(L - B)$), reflecting the need to balance economic development and ecological sustainability [7]. Technological efforts are subject to natural depletion $\left(\rho_1 T_e\right)$. Finally, equation seven models the implementation of economic measures to support livelihoods and control the exploitation of resources. The rate at which economic measures are instituted is assumed to be directly proportional to the magnitude of population pressure (ωP), reflecting the need to address social and economic dimensions of forest management [21]. Economic measures are subject to natural depletion as well $\left(\omega_1 E_f\right)$.

In addition to the dynamics of wildlife population, the functions of the intrinsic growth rate $r(B)$ and the carrying capacity $K(B)$ are given in Eqs. (2) and (3), respectively.

$$r(B) = \alpha\eta B,\ 0 \leq \eta \leq 1, \tag{2}$$

$$K(B) = K_0 + K_1 B, \tag{3}$$

such that,

$$K(0) = K_0 > 0, K'(B) > 0,\ \text{for}\ B > 0,\ \text{and}\ K_1 > 0.$$

3. Qualitative analysis

3.1. Well–posedness and boundedness of the model

When a model is well–posed it means that non–negative initial conditions lead to non–negative solutions [32]. Let

$$\mathbb{R}^7_+ = \left\{B(t), W(t), N(t), P(t), H(t), T_e(t), E_f(t)\right\}$$

be the set containing positive coordinate of $\mathbb{R}^7$. Now, consider the model system (1) has initial values

$$\mathbb{R}^7_+(0) = \left\{B(0), W(0), N(0), P(0), H(0), T_e(0), E_f(0)\right\}.$$

If

$$B(0) \geq 0,\ W(0) \geq 0,\ N(0) \geq 0,\ P(0) \geq 0,\ H(0) \geq 0,\ T_e(0) \geq 0,$$

and $E_f(0) \geq 0$,

then

$$B(t) \geq 0,\ W(t) \geq 0,\ N(t) \geq 0,\ P(t) \geq 0,\ H(t) \geq 0,\ T_e(t) \geq 0,$$

and $E_f(t) \geq 0$.

Thus, we show that $\mathbb{R}^7_+$ is positively invariant with respect to system (1) by examining the direction of the vector field on each coordinate plane. Consider the $B - W - N$: On this plane $P = H = T_e = E_f = 0$ and

$$\dot{P}\Big|_{P=H=T_e=E_f=0} = \phi N > 0, \quad \dot{H}\Big|_{P=H=T_e=E_f=0} = \gamma N > 0,$$
$$\dot{T}_e\Big|_{P=H=T_e=E_f=0} = \rho(L - B) > 0, \quad \dot{E}_f\Big|_{P=H=T_e=E_f=0} = 0.$$

Further, we take $W - N - P$ plane: On this plane $B = H = T_e = E_f = 0$ and

$$\dot{B}\Big|_{B=H=T_e=E_f=0} = 0, \quad \dot{H}\Big|_{B=H=T_e=E_f=0} = \gamma N > 0,$$
$$\dot{T}_e\Big|_{B=H=T_e=E_f=0} = \rho L > 0, \quad \dot{E}_f\Big|_{B=H=T_e=E_f=0} = 0.$$

Thus, we observe that some of the vector fields are tangents to the coordinate and others are pointing to the interior of $\mathbb{R}^7_+$ suggesting that all solutions starting in $\mathbb{R}^7_+$ remain in $\mathbb{R}^7_+$ for all $t > 0$. Hence, the system is well posed. The bounds of the variables in conservation model are stated in Lemma 1 (proof refer [19]).

Lemma 1. *The set*

$$\Omega_c = \Big\{ \big(B, W, N, P, H, T_e\big) : 0 \leq B \leq L,\ 0 \leq W \leq K(L),\ 0 \leq N \leq N_m,$$
$$0 \leq P \leq P_m,\ 0 \leq H \leq H_m,\ 0 \leq T_e \leq \frac{\rho L}{\rho_1},\ 0 \leq E_f \leq \frac{\omega}{\omega_1} P_m \Big\},$$

is the region of convergence for the model system (1), attracting all solutions that originate within the interior of the positive orthant and converge towards it. Where,

$$N_m = \frac{M}{\theta}\left(\theta + \lambda\beta_1 L\right), \quad P_m = \frac{\phi}{\phi_0} N_m, \quad \textit{and} \quad H_m = \frac{\gamma N_m + \phi_2 P_m}{\gamma_1 - \pi\beta_2 L^2},$$

with condition

$$\gamma_1 > \pi\beta_2 L^2.$$

Thus, in the region $\mathbb{R}^7_+$ the model is ecologically and mathematically well posed, hence, can be used to study the conservation of forest biomass and forest–dependent wildlife.

3.2. Equilibrium analysis

In our study, we made the assumption that wildlife species rely entirely on forest ecosystems for their survival and existence, thus, the possibility of equilibrium point $W \neq 0$ while $B = 0$ has been eliminated. Therefore, the model has five boundary equilibria and one interior equilibrium point.

$$E_1\left(0, 0, 0, 0, 0, \frac{\rho L}{\rho_1}, 0\right),\ E_2(L, 0, 0, 0, 0, 0, 0),\ E_3\left(B_3, W_3, 0, 0, 0, \frac{\rho(L - B_3)}{\rho_1}, 0\right),$$
$$E_4\left(0, 0, M, P_4, H_4, \frac{\rho L}{\rho_1}, E_{f_4}\right),\ E_5\left(B_5, 0, N_5, P_5, H_5, \frac{\rho(L - B_5)}{\rho_1}, E_{f_5}\right),$$
$$\overline{E}\left(\overline{B}, \overline{W}, \overline{N}, \overline{P}, \overline{H}, \overline{T_e}, \overline{E_f}\right),$$

where,

$$P_4 = \frac{\sqrt{(\omega_1\phi_0)^2 + 4M\omega_1\phi_1\omega\phi} - \omega_1\phi_0}{2\omega\phi_0},$$
$$E_4 = \frac{\omega P_4}{\omega_1},\ H_4 = \frac{\gamma M + \phi_2 P_4}{\gamma_1}.$$

It can be noted that existence of E_1, E_2, and E_4 is obvious. Further, the existence of E_3, E_5 and $\overline{E}$ can be shown in a similar way as in [19,20]. For quantitative analysis purpose, we show the existence of $\overline{E}$. It is worth noting that at $\overline{E}$, the values $\overline{B}$, $\overline{W}$, $\overline{N}$, $\overline{P}$, $\overline{H}$, $\overline{T_e}$ and $\overline{E_f}$ are the positive solutions of the algebraic Eqs. (4a)–(4g).

$$s\left(1-\frac{B}{L}\right)-\alpha W-\beta_1 N-\beta_2 BH+\rho_2 T_e=0, \tag{4a}$$

$$r(B)\left(1-\frac{W}{K(B)}\right)-\nu_1 N-\nu_2 H=0, \tag{4b}$$

$$\theta\left(1-\frac{N}{M}\right)+\lambda\beta_1 B-\sigma W=0, \tag{4c}$$

$$\phi N-\phi_0 P-\phi_1 E_f P=0, \tag{4d}$$

$$\gamma N+\pi\beta_2 B^2 H+\phi_2 P-\gamma_1 H=0, \tag{4e}$$

$$\rho(L-B)-\rho_1 T_e=0, \tag{4f}$$

$$\omega P-\omega_1 E_f=0. \tag{4g}$$

With proper substitutions and some algebraic manipulations on the Eqs. (4a)–(4g) we obtain the isoclines (5) and (6).

$$s\left(1-\frac{B}{L}\right)-\alpha W-\beta_1 h_1(B,W)-\beta_2 B h_3(B,W)+\frac{\rho\rho_2}{\rho_1}(L-B)=0=\mathcal{H}_1(B,W)\ \text{(Say)}. \tag{5}$$

$$r(B)\left(1-\frac{W}{K(B)}\right)-\nu_1 h_1(B,W)-\nu_2 h_3(B,W)=0=\mathcal{H}_2(B,W)\ \text{(Say)}. \tag{6}$$

Where,

$$N=\frac{M}{\theta}\left(\theta+\lambda\beta_1 B-\sigma W\right)=h_1(B,W), \tag{7}$$

N is positive provided inequality (8) is satisfied,

$$\theta+\lambda\beta_1 B>\sigma W. \tag{8}$$

$$P=\frac{\sqrt{\omega_1^2\phi_0^2+4\omega_1\omega\phi_1\phi h_1(B,W)}-\omega_1\phi_0}{2\omega\phi_0}=h_2(B,W). \tag{9}$$

$$H=\frac{\gamma h_1(B,W)+\phi_2 h_2(B,W)}{\gamma_1-B^2\pi\beta_2}=h_3(B,W), \tag{10}$$

H is positive provided condition (11) holds,

$$\gamma_1>\pi\beta_2 B^2. \tag{11}$$

$$T_e=\frac{\rho\rho_2}{\rho_1}(L-B). \tag{12}$$

$$E_f=\frac{\omega h_2(B,W)}{\omega_1}. \tag{13}$$

From the isocline (5) we infer the following:

(a) When $W=0$, gives $\mathcal{H}_1(B,0)=\mathcal{R}_1(B)$ (say).

$$s\left(1-\frac{B}{L}\right)-\beta_1 h_1(B)-\beta_2 B h_3(B)+\frac{\rho\rho_2}{\rho_1}(L-B)=\mathcal{R}_1(B) \tag{14}$$

Further, from Eq. (14), we have the following inferences,

i. When $B=0$, gives Eq. (15)

$$\mathcal{R}_1(0)=s+\frac{\rho\rho_2}{\rho_1}L-\beta_1 M, \tag{15}$$

$\mathcal{R}_1(0)$ is positive provided inequality (16) holds,

$$s+\frac{\rho\rho_2}{\rho_1}L>\beta_1 M. \tag{16}$$

ii. When $B=L$, we have

$$\mathcal{R}_1(L)=-\beta_1 h_1(L)-\beta_2 L h_3(L),$$

$\mathcal{R}_1(L)<0$ provided inequality (11) holds.

iii. The derivative of $\mathcal{R}_1(B)$ with respect to B gives

$$\mathcal{R}_1'(B) = -\frac{s}{L} - \beta_1 h_1'(B) - \beta_2 B h_3'(B) - \beta_2 h_3(B),$$

$\mathcal{R}_1'(B) < 0$ provided inequality (11) holds.

With these considerations (i–iii), we noted that Eq. (14) has a positive unique solution $\overline{B}$ in $0 < B < L$.

(b) When $W \to \infty$, $B < 0$.

(c) $\left(\frac{dW}{dB}\right)_1 < 0$ (The derivative of W with respect to B from Eq. (6)).

Similarly, from the isocline (6) we infer the following:

(a) When $W = 0$, gives $\mathcal{H}_2(B,0) = \mathcal{R}_2(B)$ (say).

$$r(B) - \nu_1 h_1(B,0) - \nu_2 h_3(B,0) = \mathcal{R}_2(B). \tag{17}$$

Furthermore, the subsequent conclusions were drawn from Eq. (17) as follows:

i. When $B = 0$, gives,

$$-\nu_1 M - \nu_2 h_3(0) < 0.$$

ii. When $B = L$, gives

$$\mathcal{R}_2(L) = r(L) - \nu_1 h_1(L) - \nu_2 h_3(L),$$

$\mathcal{R}_2(L) > 0$ if and only if

$$r(L) > \nu_1 h_1(L) + \nu_2 h_3(L).$$

iii. The derivative of $\mathcal{R}_2(B)$ with respect to B gives,

$$\mathcal{R}_2'(B) = r'(B) - \nu_1 h_1'(B) - \nu_2 h_3'(B),$$

$\mathcal{R}_2'(B) > 0$ if and only if

$$r'(B)\nu_1 h_1'(B) + \nu_2 h_3'(B).$$

Thus, these considerations ((i)–(iii)) suggesting that $\mathcal{R}_2(B)$ has a unique non–negative solution $\overline{B}$ in $0 < B < L$.

(b) When $B \to \infty$, $W > 0$.

(c) $\left(\frac{dW}{dB}\right)_2 > 0$ (The derivative of W with respect to B from Eq. (6)).

Therefore, the values of $\overline{B}$ and $\overline{W}$ are unique (see Fig. 1) in the regions $0 < B < L$ and $0 < W < K(L)$, respectively, provided

$$\left(\frac{dW}{dB}\right)_1 < 0$$

and

$$\left(\frac{dW}{dB}\right)_2 > 0.$$

The values of $\left(\frac{dW}{dB}\right)_1$ and $\left(\frac{dW}{dB}\right)_2$ are determined from Eqs. (5) and (6), respectively. Hence, once the values of $\overline{B}$ and $\overline{W}$ are known, the values of $\overline{N}$, $\overline{P}$, $\overline{H}$, $\overline{T_e}$ and $\overline{E_f}$ can be evaluated from Eqs. (7), (9), (10), (12) and (13), respectively.

3.3. Stability analysis

We used the sign of the eigenvalues of the appropriate Jacobian matrix to determine the local stability of the equilibrium point [13]. The overall Jacobian matrix (J) of the system (1) is give as

$$J = \begin{pmatrix} j_{11} & -\alpha B & -\beta_1 B & 0 & -\beta_2 B^2 & \rho_2 B & 0 \\ j_{21} & j_{22} & -\nu_1 W & 0 & -\nu_2 W & 0 & 0 \\ \lambda\beta_1 N & -\sigma N & j_{33} & 0 & 0 & 0 & 0 \\ 0 & 0 & \phi & -\left(E\phi_1 + \phi_0\right) & 0 & 0 & -\phi_1 P \\ 2H\pi\beta_2 B & 0 & \gamma & \phi_2 & -\left(\gamma_1 - \pi\beta_2 B^2\right) & 0 & 0 \\ -\rho & 0 & 0 & 0 & 0 & -\rho_1 & 0 \\ 0 & 0 & 0 & \omega & 0 & 0 & -\omega_1 \end{pmatrix}$$

where,

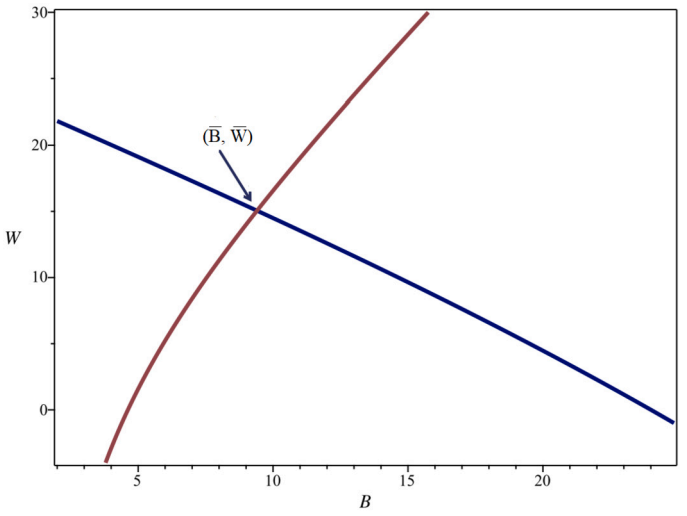

Fig. 1. The plot illustrates the intersection of isoclines (5) and (6), highlighting a distinct point $(\overline{B}, \overline{W})$ within the interior of the first quadrant.

$$j_{11} = s\left(1 - \frac{B}{L}\right) - \frac{sB}{L} - \alpha W - \beta_1 N - 2\beta_2 BH + \rho_2 T_e,$$
$$j_{21} = r'(B)W\left(1 - \frac{W}{K(B)}\right) + \frac{r(B)W^2K'(B)}{K(B)^2},$$
$$j_{22} = r(B)\left(1 - \frac{W}{K(B)}\right) - \frac{r(B)W}{K(B)} - \nu_1 N - \nu_2 H,$$
$$j_{33} = \theta\left(1 - \frac{N}{M}\right) - \frac{\theta N}{M} + \lambda\beta_1 B - \sigma W.$$

Accordingly, linear stability analysis of the equilibrium points E_1, E_2, E_3, E_4, E_5 gives the following conclusion:

(i) at E_1, the system exhibits unstable manifold locally in the direction of $B - N - P$ space;
(ii) at E_2, the system is locally unstable in $W - N - P$ plane if and only if $\gamma_1 > \pi\beta_2 L^2$;
(iii) at E_3, the system exhibits unstable behaviour in the direction of $N - P$ plane whenever $\gamma_1 > \pi\beta_2 B_3^2$;
(iv) at E_4, the system exhibits unstable behaviour in the direction of B whenever either E_5 or $\overline{E}$ exist;
(v) at E_5, the system exhibits unstable behaviour in the direction of N provided $r(B_5) > \nu_1 N_5 + \nu_2 H_5$.

The local stability behaviour of the system (1) at $\left(\overline{E}\right)$ is evaluated by using Lyapunov direct method [12] through linearising the system. Theorem 2 establishes the necessary conditions for local stability behaviour of the point $\overline{E}$.

Theorem 2. *The model system (1) exhibits local asymptotic stability at the interior equilibrium point $\overline{E}$ if exists whenever conditions (18)–(24) hold.*

$$\alpha\left(\frac{\overline{W}}{K\left(\overline{B}\right)} + \frac{r\left(\overline{B}\right)\overline{W}K'\left(\overline{B}\right)}{K\left(\overline{B}\right)^2}\right)^2 < \frac{4}{3}\left(\frac{s}{L} + \beta_2\overline{H}\right)\left(\frac{\overline{B}}{K\left(\overline{B}\right)}\right), \tag{18}$$
$$\left(\frac{\nu_1}{\eta} + \frac{\sigma}{\lambda}\right)^2 < \frac{4}{9}\left(\frac{r\left(\overline{B}\right)}{K\left(\overline{B}\right)}\right)\frac{\theta}{M\lambda}, \tag{19}$$
$$\left(\frac{\nu_2}{\eta}\right)^2 < \frac{2}{9}\left(\frac{\gamma_1 - \beta_2\pi\overline{B}^2}{\pi\overline{H}}\right)\left(\frac{\alpha\overline{B}}{K\left(\overline{B}\right)}\right), \tag{20}$$
$$\frac{\phi^2\omega}{\phi_1\overline{P}} < \frac{2\theta\left(\overline{E_f}\phi_1 + \phi_0\right)}{3M\lambda}, \tag{21}$$
$$\frac{\gamma^2}{2\pi\overline{H}} < \frac{4\theta\left(\gamma_1 - \beta_2\pi\overline{B}^2\right)}{9M\lambda}, \tag{22}$$

$$\frac{\phi_2^2}{\pi\overline{H}} < \frac{4\left(\gamma_1 - \beta_2\pi\overline{B}^2\right)\left(\overline{E_f}\phi_1 + \phi_0\right)}{3\phi_1\overline{P}}, \tag{23}$$

$$\gamma_1 > \beta_2\pi\overline{B}^2. \tag{24}$$

Proof of Theorem *(2).* To understand how the system behaves in the neighbourhood of equilibrium point $\overline{E}$, we linearise system (1) by using the following transformations:

$$B = \overline{B} + b,\ W = \overline{W} + w,\ N = \overline{N} + n,\ P = \overline{P} + p,$$

$$H = \overline{H} + h\ , T_e = \overline{T_e} + t_e\ , E_f = \overline{E_f} + e_f,$$

where b, w, n, p, h, t_e and e_f are small perturbations around the equilibrium $\overline{E}$. After carrying out some algebraic manipulations, we obtained the linearised system (25).

$$\begin{cases} \dot{b} = -\left(\dfrac{s\overline{B}}{L} + \beta_2\overline{BH}\right)b - \alpha\overline{B}w - \beta_1\overline{B}n - \beta_2\overline{B}^2h + \rho_2\overline{B}t_e, \\ \dot{w} = \left(r'\left(\overline{B}\right)\overline{W}\left(1 - \dfrac{\overline{W}}{K\left(\overline{B}\right)}\right) + \dfrac{r\left(\overline{B}\right)\overline{W}^2K'\left(\overline{B}\right)}{K\left(\overline{B}\right)^2}\right)b \\ \qquad -\left(\dfrac{r\left(\overline{B}\right)\overline{W}}{K\left(\overline{B}\right)}\right)w - \nu_1\overline{W}n - \nu_2\overline{W}h, \\ \dot{n} = \lambda\beta_1\overline{N}b - \sigma\overline{N}w - \dfrac{\theta\overline{N}}{M}n, \\ \dot{p} = \phi n - \left(\overline{E_f} + e_f\phi_1 + \phi_0\right)p - \phi_1\overline{P}e_f, \\ \dot{h} = 2\beta_2\pi\overline{BH}b + \gamma n + \phi_2 p + \left(\beta_2\pi\overline{B}^2 - \gamma_1\right)h, \\ \dot{t_e} = -\rho b - \rho_1 t_e, \\ \dot{e_f} = \omega p - \omega_1 e_f. \end{cases} \tag{25}$$

Considering the positive definite function (26) [11,19,8,7]

$$\mathcal{V} = \frac{1}{2}\left(\frac{1}{\overline{B}}b^2 + \frac{\kappa_1}{\overline{W}}w^2 + \frac{\kappa_2}{\overline{N}}n^2 + \kappa_3 p^2 + \kappa_4 h^2 + \kappa_5 t_e^2 + \kappa_6 e_f^2\right), \tag{26}$$

where κ_1, κ_2, κ_3, κ_4, κ_5 and κ_6 are positive constants. Equilibrium point $\overline{E}$ is locally asymptotic stable provided the time derivative of Eq. (26) at $\overline{E}$ is negative. By taking the time derivative of Eq. (26) with respect to the solution of the linearised system (25), we obtain:

$$\begin{aligned} \frac{d\mathcal{V}}{dt} = &-\left(\frac{s}{L} + \beta_2\overline{H}\right)b^2 - \alpha bw - \beta_1 bn - \beta_2\overline{B}bh + \rho_2 bt_e - \kappa_1\left(\frac{r\left(\overline{B}\right)}{K\left(\overline{B}\right)}\right)w^2 \\ &-\kappa_1\nu_1 wn - \kappa_1\nu_2 wh + \kappa_1\left(r'\left(\overline{B}\right)\left(1 - \frac{\overline{W}}{K\left(\overline{B}\right)}\right) + \frac{r\left(\overline{B}\right)\overline{W}K'\left(\overline{B}\right)}{K\left(\overline{B}\right)^2}\right)bw \\ &+\kappa_2\lambda\beta_1 bn - \kappa_2\sigma nw - \frac{\kappa_2\theta}{M}n^2 + \kappa_3\phi np - \kappa_3\left(\phi_0 + \phi_1\overline{E_f}\right)p^2 - \kappa_3\phi_1\overline{P}e_f p \\ &+2\kappa_4\beta_2\pi\overline{B}\,\overline{H}bh + \kappa_4\gamma nh + \kappa_4\phi_2 ph + \kappa_4\left(\beta_2\pi\overline{B}^2 - \gamma_1\right)h^2 - \kappa_5\rho bt_e - \kappa_5\rho_1 t_e^2 \\ &+\kappa_6\omega pe_f - \kappa_6\omega_1 e_f^2, \end{aligned}$$

choosing

$$\kappa_1 = \frac{1}{\eta},\quad \kappa_2 = \frac{1}{\lambda},\quad \kappa_3 = \frac{\omega}{\phi_1\overline{P}},\quad \kappa_4 = \frac{1}{2\pi\overline{H}},\quad \kappa_5 = \frac{\rho_2}{\rho} \text{ and } \quad \kappa_6 = 1,$$

$\dfrac{d\mathcal{V}}{dt}$ is reduced to

$$= -\left(\frac{s}{L} + \beta_2 \overline{H}\right) b^2 - \kappa_1 \left(\frac{r\left(\overline{B}\right)}{K\left(\overline{B}\right)}\right) w^2 - \frac{\kappa_2 \theta}{M} n^2 - \kappa_3 \left(\phi_1 \overline{E_f} + \phi_0\right) p^2$$

$$- \kappa_4 \left(\gamma_1 - \beta_2 \pi \overline{B}^2\right) h^2 - \kappa_5 \rho_1 t_e^2 - \kappa_6 \omega_1 e_f^2 - \kappa_1 \left(\frac{\overline{W}}{K\left(\overline{B}\right)} + \frac{r\left(\overline{B}\right) \overline{W} K'\left(\overline{B}\right)}{K\left(\overline{B}\right)^2}\right) bw$$

$$- (\kappa_1 \nu_1 + \kappa_2 \sigma) wn - \kappa_1 \nu_2 wh + \kappa_3 \phi np + \kappa_4 \gamma nh + \kappa_4 \phi_2 ph.$$

It can be noted that $\frac{d\mathcal{V}}{dt}$ is negative definite provided Eqs. (18)–(24) are satisfied.

Furthermore, it is imperative to show $\overline{E}$ is also globally asymptotically stable. Theorem 3 provides sufficient conditions for global stability behaviour of equilibrium point $\overline{E}$.

Theorem 3. *The system (1) exhibits global asymptotic stable behaviour at $\overline{E}$ in the region Ω_c provided inequalities (27)–(34) hold.*

$$\alpha \left(\left(LK(L)\Gamma(L)\right) + \frac{\overline{W}}{K\left(\overline{B}\right)}\right)^2 < \frac{2}{3}\left(\frac{s}{L} + \beta_2 \overline{H}\right) \frac{L}{K\left(\overline{B}\right)}, \tag{27}$$

$$\pi \overline{H} \left(\beta_2 \overline{B}\right)^2 < \frac{2}{3}\left(\frac{s}{L} + \beta_2 \overline{H}\right)\left(\gamma_1 - \pi \beta_2 L^2\right), \tag{28}$$

$$\left(\frac{\nu_1}{\eta} + \frac{\sigma}{\lambda}\right)^2 < \frac{4\alpha\theta L}{9\lambda M K\left(\overline{B}\right)}, \tag{29}$$

$$\left(\nu_2\right)^2 < \frac{4\alpha\eta^2 L\left(\gamma_1 - \pi\beta_2 L^2\right)}{9\pi \overline{H} K\left(\overline{B}\right)}, \tag{30}$$

$$\frac{\omega\phi^2}{\phi_1 \overline{P}} < \frac{2}{3}\frac{\theta}{\lambda M}\left(\phi_0 + \frac{\omega\phi P_m}{\omega_1}\right), \tag{31}$$

$$\frac{\gamma^2}{\pi \overline{H}} < \frac{4\theta\left(\gamma_1 - \pi\beta_2 L^2\right)}{\lambda M}, \tag{32}$$

$$\frac{\phi_2^2}{\pi \overline{H}} < \frac{2\left(\gamma_1 - \pi\beta_2 L^2\right)}{3\lambda}\frac{\omega\phi P_m}{\omega_1}, \tag{33}$$

$$\gamma_1 > \pi \beta_2 L^2. \tag{34}$$

Proof of Theorem *(3).* Consider positive definite function (35) about $\overline{E}$,

$$\begin{aligned}\mathcal{U} = &\left(B - \overline{B} - \overline{B}\ln\frac{B}{\overline{B}}\right) + m_1\left(W - \overline{W} - \overline{W}\ln\frac{W}{\overline{W}}\right)\\ &+ m_2\left(N - \overline{N} - \overline{N}\ln\frac{N}{\overline{N}}\right) + \frac{m_3}{2}\left(P - \overline{P}\right)^2\\ &+ \frac{m_4}{2}\left(H - \overline{H}\right)^2 + \frac{m_5}{2}\left(T_e - \overline{T_e}\right)^2 + \frac{m_6}{2}\left(E_f - \overline{E_f}\right)^2,\end{aligned} \tag{35}$$

where, m_1, m_2, m_3 m_4, m_5 and m_6 are positive constants. We observed that the function $\mathcal{U}$ is positive definite by showing that $\mathcal{U}(B, W, N, P, H, T_e, E_f) > 0$ in the interior of Ω_c and $\mathcal{U}(B, W, N, P, H, T_e, E_f) = 0$ only at $\overline{E}$. Now, for $y^* > 0$, let $g(y) = (y - y^*) - y^* \ln\frac{y}{y^*}$, then $g(y^*) = 0$ and $g'(y) = 1 - \frac{y}{y^*}$. Thus, $g'(y) > 0$ when $y < y^*$ and $g'(y) < 0$ when $y > y^*$, suggesting that the function $g(y)$ has an absolute minimum 0 at $y = y^*$ in the interval $(0, \infty)$. This property implies that the function $\mathcal{U}$ is positive definite with respect to $\overline{E}$, thus, we used the function to study the behaviour of the system at $\overline{E}$ globally. The time derivative of Eq. (35) gives

$$\begin{aligned}\frac{d\mathcal{U}}{dt} = &\left(\frac{B - \overline{B}}{B}\right)\frac{dB}{dt} + m_1\left(\frac{W - \overline{W}}{W}\right)\frac{dW}{dt}\\ &+ m_2\left(\frac{N - \overline{N}}{N}\right)\frac{dN}{dt} + m_3\left(P - \overline{P}\right)\frac{dP}{dt}\\ &+ m_4\left(H - \overline{H}\right)\frac{dH}{dt} + m_5\left(T_e - \overline{T_e}\right)\frac{dT_e}{dt}\\ &+ m_6\left(E_f - \overline{E_f}\right)\frac{dE_f}{dt}.\end{aligned}$$

Substituting the values of $\frac{dB}{dt}$, $\frac{dW}{dt}$, $\frac{dN}{dt}$, $\frac{dP}{dt}$, $\frac{dH}{dt}$, $\frac{dT_e}{dt}$ and $\frac{dE_f}{dt}$ from the system (1) and choosing $m_1 = \frac{1}{\eta}$, $m_2 = \frac{1}{\lambda}$, $m_3 = \frac{\omega}{\phi_1 \overline{P}}$, $m_4 = \frac{1}{\pi \overline{H}}$, $m_5 = \frac{\rho_2}{\rho}$, and $m_6 = 1$, $\frac{d\mathcal{U}}{dt}$ is reduced to

$$\begin{aligned}
\frac{d\mathcal{U}}{dt} &= \left(B-\overline{B}\right)\left[-\left(\frac{s}{L}+\beta_2\overline{H}\right)\left(B-\overline{B}\right)\right] \\
&+m_1\left(W-\overline{W}\right)\left[-\frac{\alpha\eta B}{K(\overline{B})}\left(W-\overline{W}\right)-\nu_1\left(N-\overline{N}\right)-\nu_2\left(H-\overline{H}\right)\right] \\
&+m_1\left(W-\overline{W}\right)\left[\left((\alpha\eta BW\Gamma(B))+\left(\frac{\alpha\eta\overline{W}}{K\left(\overline{B}\right)}\right)\right)\left(B-\overline{B}\right)\right] \\
&+m_2(N-\overline{N})\left[-\frac{\theta}{M}\left(N-\overline{N}\right)\right]+m_2(N-\overline{N}\left[-\sigma\left(W-\overline{W}\right)\right] \\
&+m_3\left(P-\overline{P}\right)\left[\phi\left(N-\overline{N}\right)-\left(\phi_0+\phi_1E_f\right)\left(P-\overline{P}\right)\right] \\
&+m_4\left(H-\overline{H}\right)\left[-\left(\gamma_1-\pi\beta_2B^2\right)\left(H-\overline{H}\right)+\gamma\left(N-\overline{N}\right)+\phi_2\left(P-\overline{P}\right)\right] \\
&+m_4\left(H-\overline{H}\right)\left[\pi\beta_2\overline{BH}\left(B-\overline{B}\right)\right]-m_5\rho_1\left(T_e-\overline{T_e}\right)^2-m_6\omega_1\left(E_f-\overline{E_f}\right)^2,
\end{aligned}$$

where,

$$\Gamma(B)=\begin{cases}\dfrac{\frac{1}{K(B)}-\frac{1}{K\left(\overline{B}\right)}}{B-\overline{B}}, & B\neq\overline{B}\\[2ex] \dfrac{-K'(B)}{\left(K\left(\overline{B}\right)\right)^2}, & B=\overline{B}\end{cases}$$

Equilibrium point $\overline{E}$ exhibits global asymptotic behaviour if the time derivative $\mathcal{U}'$ at point $\overline{E}$ is negative definite. Hence, it is noteworthy that $\mathcal{U}'$ is negative definite in the region of attraction Ω_c under conditions (27)–(34).

4. Quantitative analysis

4.1. Parameter estimation and model fitting

After understanding the asymptotic behaviours and long–term qualitative results of the model system, parameter estimation is crucial for obtaining accurate quantitative predictions over a finite time period when the problem is limited by real data [32]. In this study, we utilised the least squares method for parameter estimation, which is suitable for general parameter estimation rather than hypothesis testing or confidence interval establishment [33]. The values (see Table A.1) were obtained by minimizing the sum of the squares of residuals $\left(\min\sum_{i=1}^{n}\left(Y_g-Y_l\right)^2\right)$ between solutions of the model (Y_l) by using the literature values and the synthetic data (Y_g) generated randomly by adding Gaussian noise to the model output (Y_l) [32]. We take the advantage of the MATLAB built–in function *(fminserch)* which uses Nelder–Mead simplex algorithm [34] to obtain the local minimisers of the residual sum of squares. The selection of initial parameter values was based on meeting the conditions outlined in the qualitative analysis. The estimated parameter values were used to fit the data (Y_g), and the resulting best fits are shown in Figs. 2(a)–2(g). Furthermore, we examined autocorrelation of the residuals and the results show that the residuals exhibit insignificant correlation at a 5% level (see Figs. 3(a)–3(g)). These findings signify that the estimated parameters yield the best fit for the data.

4.2. Uncertainty and Sensitivity (US) analysis

Uncertainty and Sensitivity (US) analysis was carried out to quantify the uncertainty of the values of the input model parameter and to determine how changes in the values affect the value of model outputs [35]. To incorporate the uncertainty in the model parameters, we applied the Latin Hypercube Sampling (LHS) technique, considering the parameters as probabilistic variables uniformly distributed across the specified ranges as indicated in Table A.2 [28]. In order to understand the impact of input uncertainty on model outputs, we performed sensitivity analysis of model outputs with respect to the model parameters using the Partial Rank Correlation Coefficient (PRCC) method [17]. A positive PRCC value indicates a positive correlation between the input parameter and the model output, meaning that as the value of the input parameter increases, the model output tends to increase, and as the value of the input parameter decreases, the model output tends to decrease. Conversely, a negative PRCC value suggests an inverse correlation between the input parameter and the model output, meaning that as the value of the input parameter increases, the model output tends to decrease, and as the value of the input parameter decreases, the model output tends to increase. The assumption of monotonicity

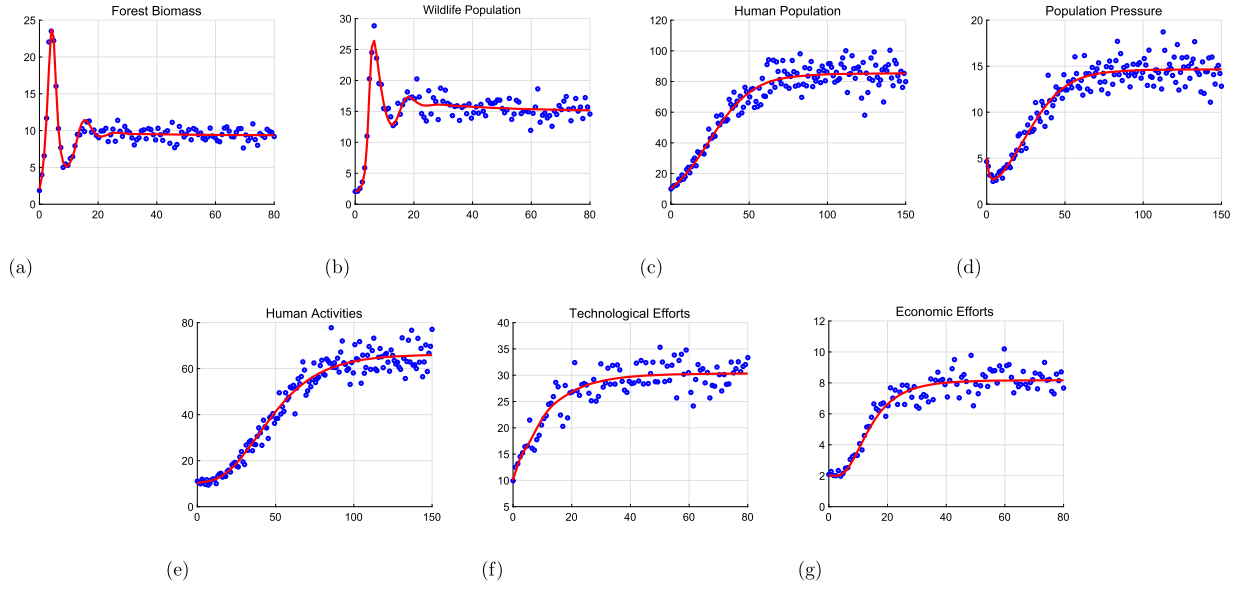

Fig. 2. Model fitting (lines) corresponding to estimated parameter values for (a) Forest biomass (b) Wildlife population (c) Human population (d) population pressure (e) Human activities (f) Technological efforts (g) Economic efforts.

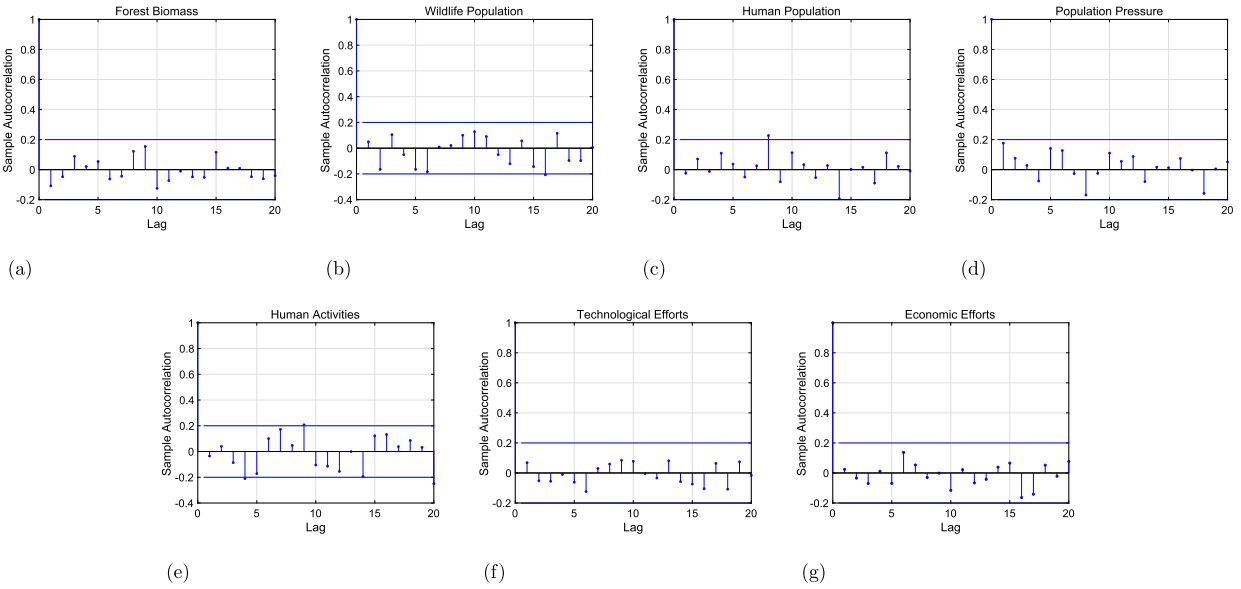

Fig. 3. The sample autocorrelation of the residuals in relation to (a) Forest biomass, (b) Wildlife population, (c) Human population, (d) Population pressure, (e) Human activities, (f) Technological efforts, and (g) Economic efforts, indicating the lack of significance at the 5% level.

between the model outputs and parameters over time was verified, and a sample of monotonicity plots is shown in Figs. 4(a)–4(f) for illustration.

An exploratory analysis was carried out using time varying sensitivity analysis, as no specific time periods of interest were identified for the study. The analysis sought to identify meaningful time–dependent correlations spanning the entire time period under investigation [15]. The sensitivity of input parameters on the density of forest biomass, wildlife population, population pressure, and human activities was determined by plotting the PRCC values computed at various time intervals against time. The results of the analysis are presented in Figs. 5(a)–5(d) From this figure, the shaded region represents PRCCs that are insignificantly different from zero ($-0.3 \leq \text{PRCC} \leq 0.3$) [15]. We observed that for forest biomass (B) and forest–dependent wildlife (W), the significant parameters throughout the entire time span are the growth rate of technological efforts (ρ), forest growth rate due to technological efforts (ρ_2), and forest depletion rate due to human activities (β_2), as their PRCC values are significantly different from zero. The positive

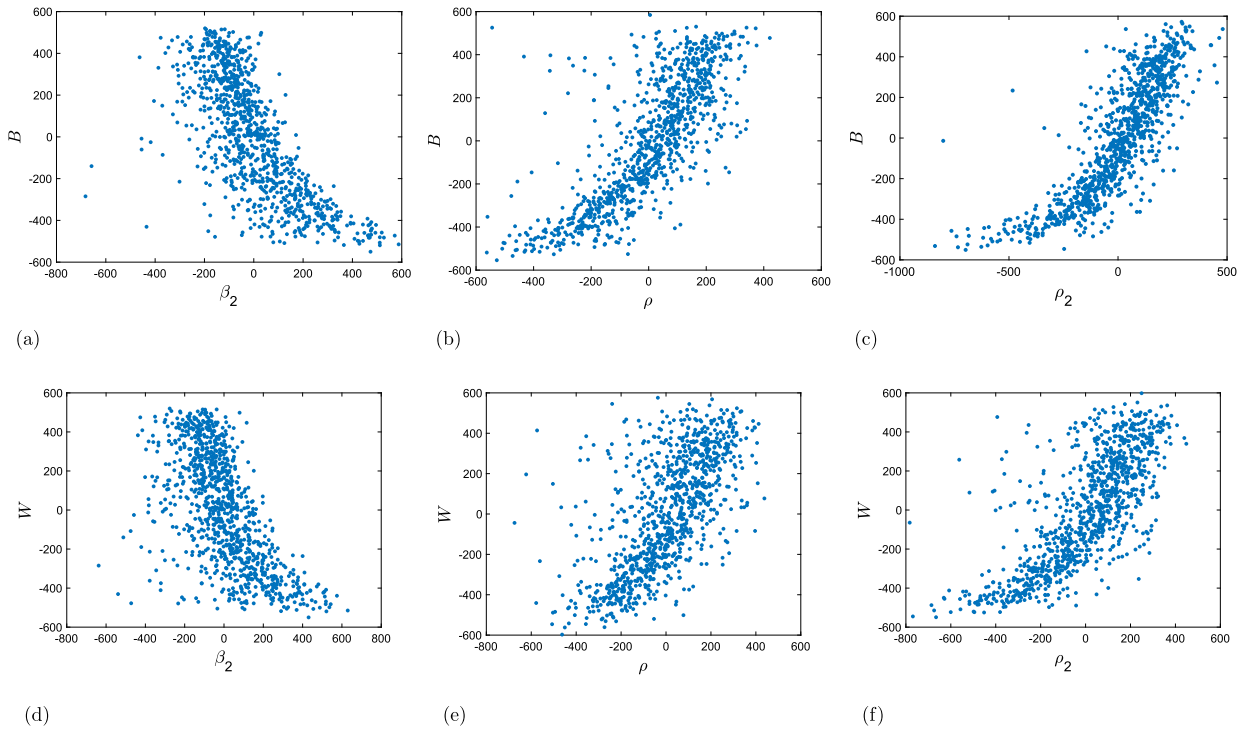

Fig. 4. Linear–linear plots of the residuals of the linear regressions of the selected LHS sampled parameters against all other parameters [abscissa] and the residuals of the linear regression of forest biomass $B(t)$ versus (a) β_2, (b) ρ, (c) ρ_1 [ordinate], and wildlife population $W(t)$ versus (d) β_2 (e) ρ and (f) ρ_2 [ordinate] computed at $t = 8$.

PRCC values for ρ and ρ_2 indicate that an increase in these parameters will increase the density of forest biomass leading to an increase in the density of forest–dependent wildlife population. Conversely, the negative PRCC value for β_2 suggests that any efforts to decrease the rate of forest depletion due to human activities will increase the density of forest biomass and forest–dependent wildlife population. Parameters such as natural depletion rate of human activities (γ_1), natural depletion rate of technological efforts (ρ_1) and human activities growth rate due to population pressure (ϕ_2) are insignificant at the early time points. This implies that any attempts to control these parameters it is not advisable to be implemented at the initial stages. For human activities (H) the sensitive parameters for the entire time span are growth rate of human population (θ), growth rate of human activities due to human population (γ), natural depletion rate of human activities (γ_1), depletion rate of population pressure due to implementation of economic measures (ϕ_1) and growth rate of human activities due to population pressure (ϕ_2). A decrease in human activities is expected if efforts are made to reduce the values of θ, γ and ϕ_2 based on the positive PRCC values associated with them. Conversely, an increase in the application of economic measures would result in a decrease in human activities due to the negative PRCC value of ϕ_1. In the context of population pressure (P), the identified significant parameters over the entire time span are human population growth rate (θ), growth rate of population pressure (ϕ), depletion rate of population pressure due to economic measures (ϕ_1), growth rate of economic measures (ω), and natural depletion rate of economic measures (ω_1). These findings suggest that policies aimed at controlling population growth or implementing economic measures to curb the growth of population pressure should be carefully evaluated and implemented over a prolonged time frame.

Similarly, we extended the sensitivity analysis by considering the time invariant of the system dynamics. When $t = 8$, representing an early time point in the system dynamics, and $t = 80$, representing a later time point, the two specific time points were arbitrarily selected. The results are shown in Figs. 6(a)–6(d) and Figs. 7(a)–7(d), and they are consistent with the time–varying sensitivity analysis.

Furthermore, we performed significance tests to determine whether the PRCC values for the two parameters in relation to forest biomass B varied significantly. Since the value of the PRCC can take any value from -1 to 1, before computing the p–values, we performed the Fisher transformation [29] to address the skewness in the distribution. The pairwise comparison was carried out for parameters whose PRCCs differed from zero significantly ($p<0.05$), the null hypothesis of no significant difference was tested for the compared sensitive parameters. The computed p–values between the compared parameters are presented in Table A.3. Further, the False Discovery Rate (FDR) adjusted p–values (see Table A.4) are computed to reduce the chance of making a Type 1 statistical error [36]. The p–values that are less than 0.05 are regarded as significantly different, and thus we fail to reject the null hypothesis. Utilising the results in Table A.4, the results of the pairwise comparison are presented in Table A.5, whereby the output is “TRUE” when the compared PRCCs values are observed to be significantly different ($p<0.05$) and “FALSE” when they are insignificantly different ($p>0.05$), thus rejecting the null hypothesis. We observed that the most of the sensitive parameters also differ significantly.

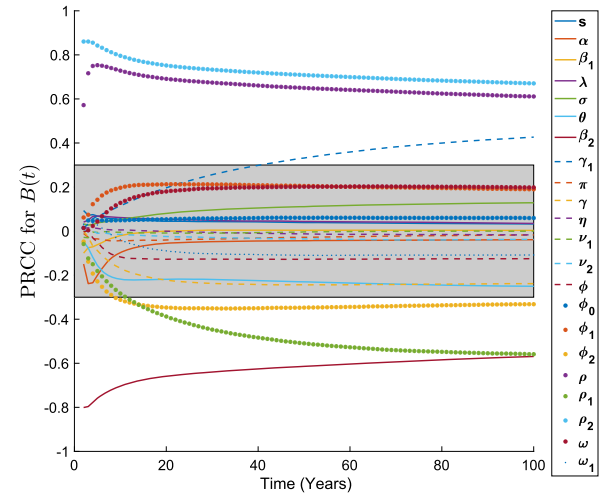

(a)

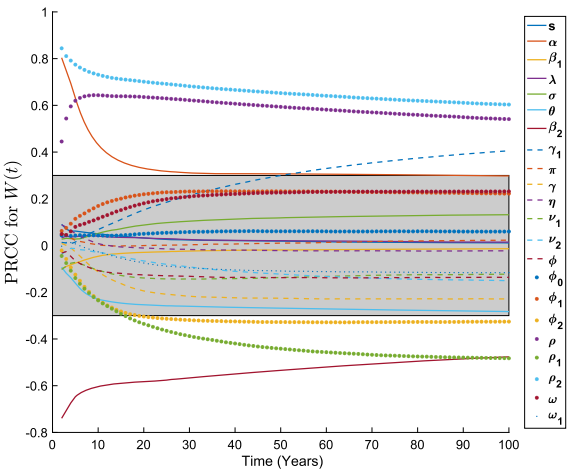

(b)

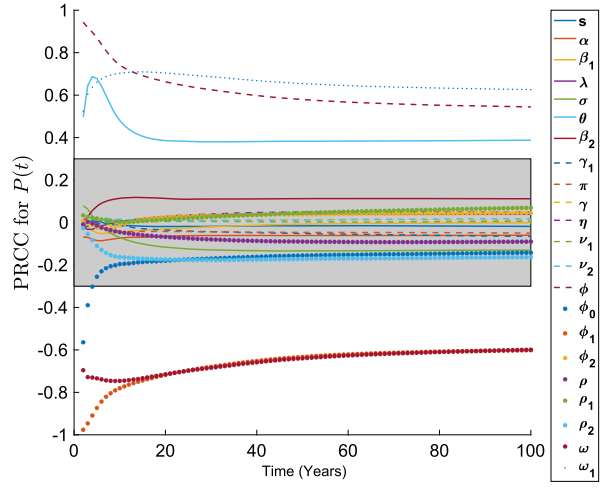

(c)

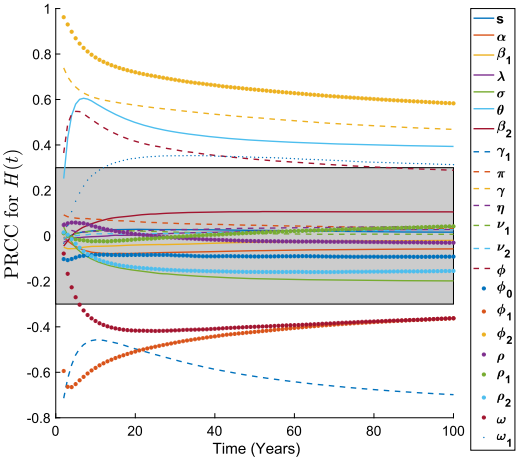

(d)

Fig. 5. A visual representation showcasing the evolution of parameter sensitivity throughout the progression of the system dynamics. PRRC values over time span of 100 years with respect to (a) forest biomass, $B(t)$ (b) forest–dependent wildlife population, $W(t)$ (c) population pressure, $P(t)$ and (d) human activities, $H(t)$.

The time variations of forest biomass, population pressure, and human activities when technological efforts (ρ) and economic measures (ω) are in place versus when they are not are shown in Figs. 8(a)–8(c). From this figure we observed that technological efforts increase the density of forest biomass, while economic measures reduce the intensity of population pressure, ultimately leading to decrease in human activities.

5. Discussion and conclusion

The need to conserve forest resources while meeting the demands for forest products may not be overemphasised. Studies consistently show that the continuous increase in human population and the corresponding increase in human activities exert significant pressure on both the intrinsic growth rate and carrying capacity of forests. The increase in human population size and its associated activities motivate more people to move into the forest areas for the purpose of establishing settlements, agricultural lands, and different economic activities. This paper explores the conservation of forest biomass and wildlife species that are reliant on forest ecosystems, considering the dynamics of human population and its associated activities. The study proposed the use of economic measures such as property rights, market charge systems, fiscal instruments, and livelihood support to reduce population pressure on forest resources. These economic measures serve the dual purpose of meeting the livelihood needs of individuals dependent on forest resources while concurrently alleviating the pressure exerted on these resources. Moreover, technological efforts are being proposed to enhance forest biomass density. These efforts involve the utilisation of drones in the seeding process and the adoption

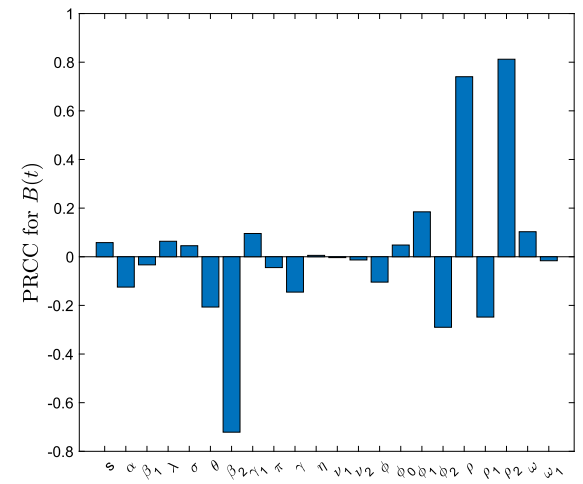

(a)

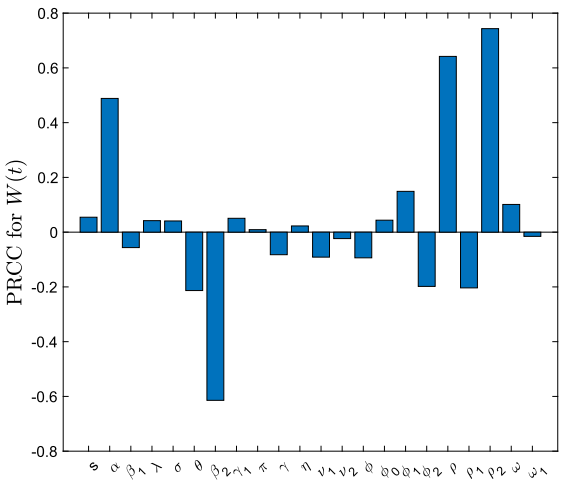

(b)

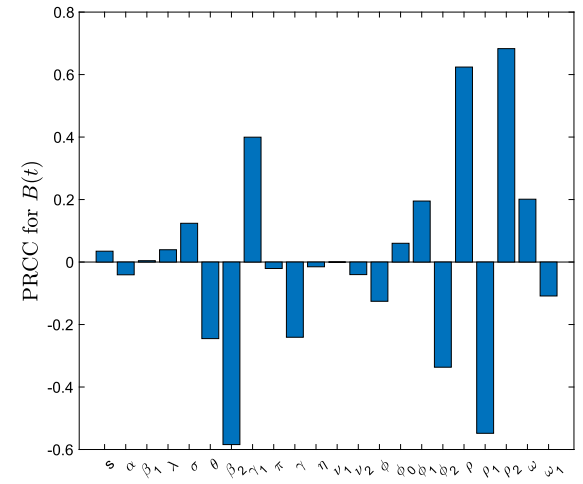

(c)

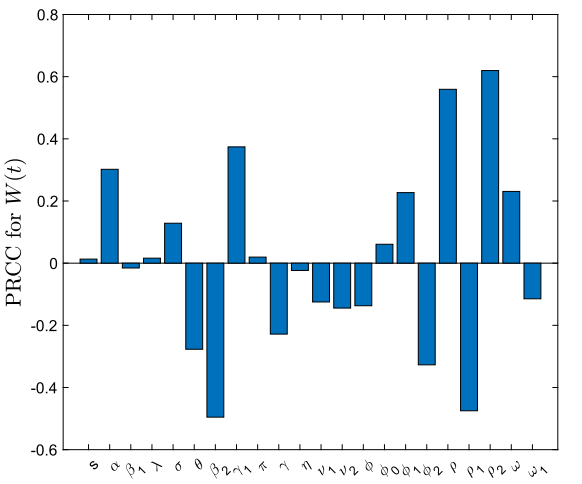

(d)

Fig. 6. The sensitivity analysis of the dynamics of the model output for $n = 1000$ simulations with time constancy. PRRCs values with respect to (a) forest biomass, $B(t)$ (b) forest–dependent wildlife population, $W(t)$ at $t = 8$ (c) forest biomass $B(t)$ and (d) forest–dependent wildlife population, $W(t)$ at $t = 80$.

of genetically modified seeds that exhibit resilience to adverse environmental conditions and accelerated growth, thereby increasing the overall density of forest biomass. The analysis of the model was conducted using the stability theory of differential equations which reveals six non–negative equilibrium points. While the local stability of the interior equilibrium point was not immediately evident, we established the conditions for both local and global stability of the interior equilibrium point by employing the theory of Lyapunov function.

Furthermore, we conducted uncertainty and sensitivity analysis using the Latin Hypercube Sampling (LHS) and Partial Rank Correlation Coefficient (PRCC) method, which is a correlation–based approach to assess the impact of input model parameter uncertainty on model outputs. Our findings indicate that some of the most sensitive parameters include the implementation rate of economic measures (ω), depletion rate of population pressure due to economic measures (ϕ_1), implementation rate of technological efforts (ρ), and growth rate of forest biomass due to application of technology (ρ_2). These results suggest that the management measures proposed in our study could be valuable for achieving sustainable forest management while satisfying the demands of the human population for forest resources. Nevertheless, the fact that these parameters are sensitive over the entire time span suggests that the measures should be evaluated and implemented over a prolonged time frame. This would allow for a comprehensive assessment of their effectiveness in achieving sustainable forest management. Furthermore, despite the fact that both economic and technological efforts have demonstrated to be potential measures, these efforts can only be used to a limited extent. The stability analysis of the

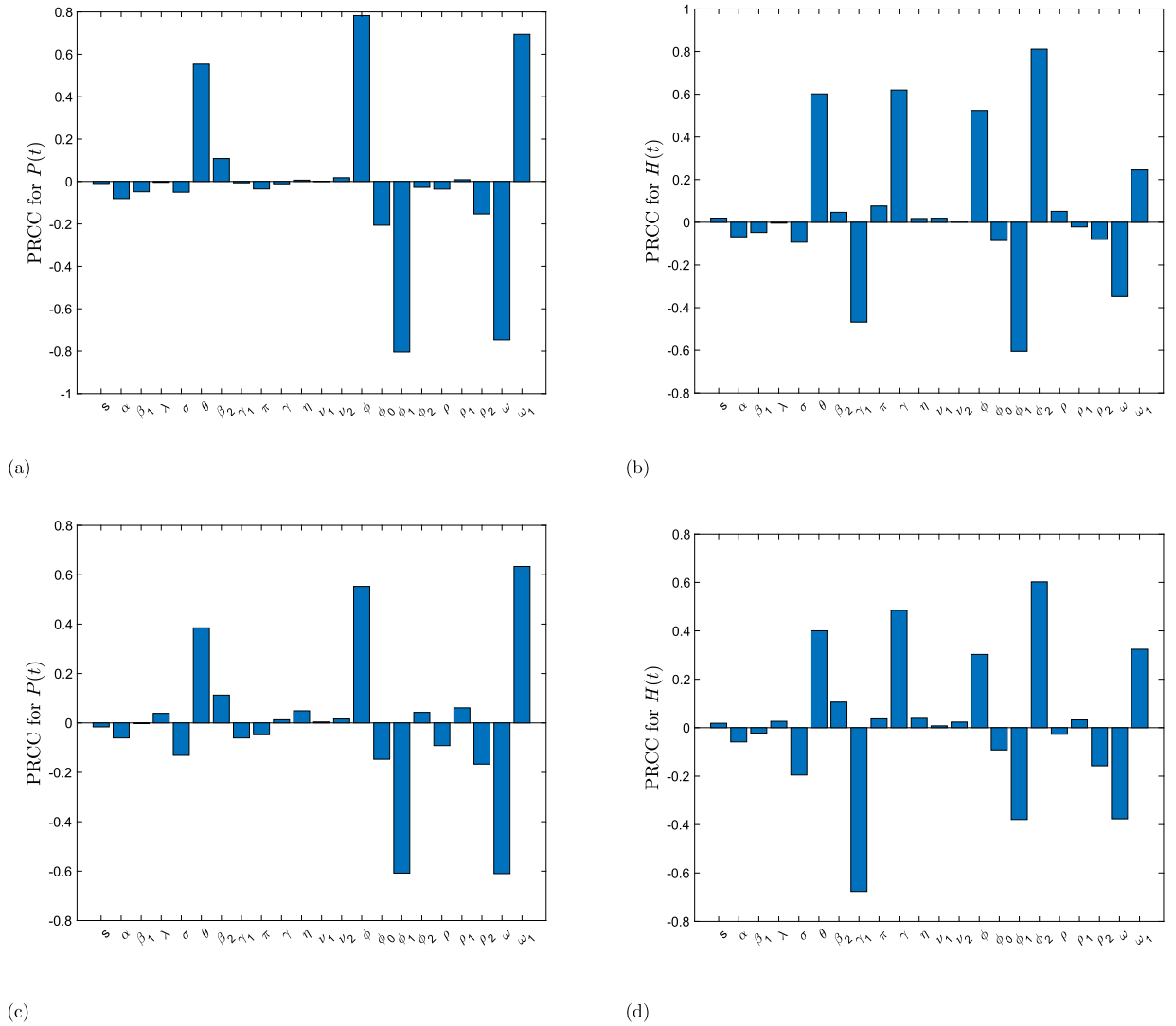

Fig. 7. The time–invariant sensitivity analysis of the dynamics of the model for $n = 1000$ simulations. PRRCs values with respect to (a) population pressure, $P(t)$ (b) human activities, $H(t)$ at $t = 8$ (c) population pressure, $P(t)$ and (d) human activities, $H(t)$ at $t = 80$.

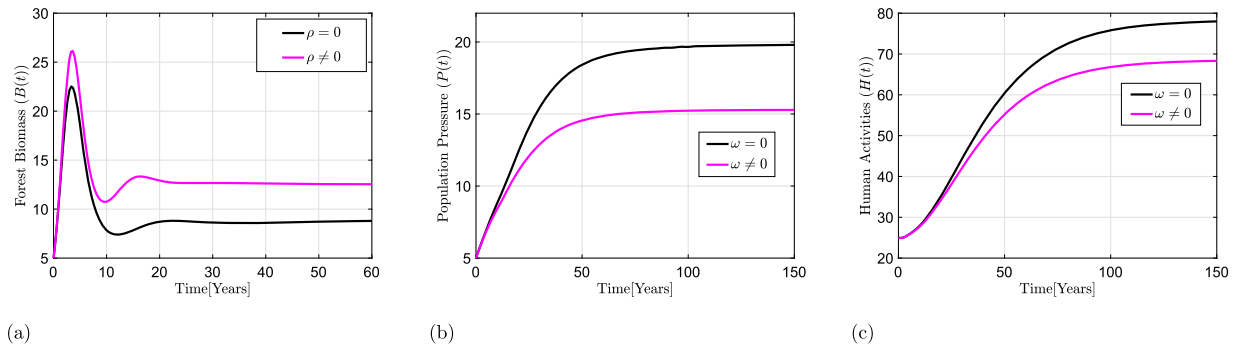

Fig. 8. Impact of technological efforts to increase the density of forest biomass and economic measures to reduce the intensity of population pressure. Variations of (a) forest biomass with time when there is no technological efforts ($\rho = 0$) and when are in place ($\rho \neq 0$) (b) population pressure with time when no economic measures are applied ($\omega = 0$) and when are in place ($\omega \neq 0$) (c) human activities with time when no economic measures are applied ($\omega = 0$) and when are in place ($\omega \neq 0$).

interior equilibrium provides conditions that must be met for the system to be stable, further attempts to apply measures that violate the stability conditions will destabilise the system.

Overall, our uncertainty and sensitivity analysis using the LHS/PRCC method provides valuable insights into the most significant parameters, which can inform forest management policies aimed at balancing ecological, social, and economic objectives. However, the approach assumes input model parameters and model output exhibit monotonicity and non–linear relationship which may not hold true in certain scenarios. To obtain a more comprehensive evaluation of model uncertainties, future research could combine the approach with other sensitivity indices such as variance–based methods (e-FAST and Sobol) that do not require the assumption of monotonicity. By combining these approaches, we might gain a better understanding of how specific parameter changes impact the output variability, however, the issue of computational costs should be taken into account as most of the variance–based methods are prone to computational resources [15].

CRediT authorship contribution statement

Ibrahim M Fanuel, Francis Moyo: Conceived and designed the experiments; performed the experiments; analyzed and interpreted the data; contributed reagents, materials, analysis tools or data; and wrote the paper.

Silas Mirau, Damian Kajunguri: Conceived and designed the experiments; performed the experiments; analyzed and interpreted the data and contributed reagents, materials, analysis tools or data.

Declaration of competing interest

The authors declare that they have no known competing financial interests or personal relationships that could have appeared to influence the work reported in this paper.

Data availability statement

The data that has been used is confidential.

Appendix A. Tables

Table A.1
Estimated parameter values.

Parameter	Initial value	Source	Estimated values	Parameter	Initial value	Source	Estimated values
s	0.8	[7]	0.69	ϕ_0	0.5	[11]	0.4323
α	0.05	[13]	0.0487	ϕ	0.1	[11]	0.09
η	0.9	[13]	0.8045	ϕ_1	0.01	[37]	0.011
β_1	0.003	[20]	0.0029	ϕ_2	0.2	Assumed	0.18
β_2	0.0004	Assumed	0.0004	ρ	0.01	[38,11]	0.028
ν_1	0.002	[20]	0.002	ρ_1	0.03	[38,11]	0.0738
ν_2	0.0001	[20]	0.0001	ρ_2	0.02	[11]	0.0215
θ	0.5	[20]	0.75	ω	0.05	[37]	0.0524
λ	0.05	[20]	0.045	ω_1	0.1	[11]	0.1067
σ	0.001	[20]	0.0012	π	0.002	[20]	0.023
γ	0.004	Assumed	0.0039	γ_1	0.01	[20]	0.0429

Table A.2
Mean values and ranges of parameters values used in LHS.

Parameter	Range	Mean value	Source	Parameter	Range	Mean value	Source
s	[0.01 – 1]	0.69	Fitted	π	[0 – 1]	0.023	Fitted
L	–	100	[7]	γ	$[10^{-4} – 0.4]$	0.0039	Fitted
α	$[10^{-4} – 0.09]$	0.0487	Fitted	γ_1	$[10^{-3} – 0.05]$	0.0429	Fitted
η	[00.8045– 1]	0.8045	Fitted	ϕ_0	[0.01 – 0.9]	0.4323	Fitted
β_1	$[10^{-4} – 0.3]$	0.0029	Fitted	ϕ	[0.01 – 0.9]	0.09	Fitted
β_2	$[10^{-5} – 0.04]$	0.0004	Fitted	ϕ_1	$[10^{-4} – 0.5]$	0.011	Fitted
ν_1	$[2\times10^{-4} – 0.2]$	0.002	Fitted	ϕ_2	[0.02 – 0.9]	0.18	Fitted
ν_2	$[2\times10^{-5} – 0.1]$	0.0001	Fitted	ρ	[0.01 – 0.8]	0.028	Fitted
θ	[0.01 – 1]	0.75	Fitted	ρ_1	$[10^{-3} – 0.5]$	0.0738	Fitted
M	–	100	[7]	ρ_2	$[10^{-4} – 0.6]$	0.0215	Fitted
K_0	–	20	[13]	ω	[0.01 – 0.5]	0.0524	Fitted
K_1	–	3	[13]	ω_1	[0.003 – 0.8]	0.1067	Fitted
λ	[0 – 1]	0.045	Fitted	σ	$[10^{-3} – 0.1]$	0.0012	Fitted

Table A.3
Pairwise PRCC comparisons (unadjusted p-values).

	β_2	θ	γ_1	γ	ϕ	ϕ_1	ϕ_2	ρ	ρ_1	ρ_2	ω	ω_1
β_2		6.80e-11	0	1.36e-11	0	0	1.50e-05	0	0.12	0	0	0
θ			0	0.81	0.006	0	0.028	0	6.61e-16	0	0	0.002
γ_1				0	0	9.3e-07	0	2.21e-11	0	2.21e-11	9.336e-07	0
γ					0.011	0	0.015	0	0	0	0	0.005
ϕ						1.31e-13	7.077e-07	0	0	0	1.31e-13	0.8215
ϕ_1							0	0	0	0	1	7.037e-13
ϕ_2								0	4.40e-09	0	0	2.163e-07
ρ									0	1	0	0
ρ_1										0	0	0
ρ_2											0	0
ω												7.037e-13
ω_1												

Table A.4
Pairwise PRCC comparisons (FDR adjusted p-values).

	β_2	θ	γ_1	γ	ϕ	ϕ_1	ϕ_2	ρ	ρ_1	ρ_2	ω	ω_1
β_2		9.13e-11	0	1.95e-11	0	0	1.753e-05	0	0.1332	0	0	0
θ			0	0.84	0.006	0	0.030	0	1.072e-15	0	0	0.003
γ_1				0	0	1.141e-06	0	3.04e-11	0	3.04e-11	1.141e-06	0
γ					0.01269	0	0.016	0	0	0	0	0.006
ϕ						2.025e-13	8.982e-07	0	0	0	2.0e-13	0.8472
ϕ_1							0	0	0	0	1	1.03e-12
ϕ_2								0	5.81e-09	0	0	2.7e-07
ρ									0	1	0	0
ρ_1										0	0	0
ρ_2											0	0
ω												1.03e-12
ω_1												

Table A.5
Parameters different after FDR adjustment?

	β_2	θ	γ_1	γ	ϕ	ϕ_1	ϕ_2	ρ	ρ_1	ρ_2	ω	ω_1
β_2		TRUE	TRUE	TRUE	TRUE	TRUE	TRUE	TRUE	FALSE	TRUE	TRUE	TRUE
θ			TRUE	FALSE	TRUE	TRUE	TRUE	TRUE	TRUE	TRUE	TRUE	TRUE
γ_1				TRUE	TRUE	TRUE	TRUE	TRUE	TRUE	TRUE	TRUE	TRUE
γ					TRUE	TRUE	TRUE	TRUE	TRUE	TRUE	TRUE	TRUE
ϕ						TRUE	TRUE	TRUE	TRUE	TRUE	TRUE	FALSE
ϕ_1							TRUE	TRUE	TRUE	TRUE	FALSE	TRUE
ϕ_2								TRUE	TRUE	TRUE	TRUE	TRUE
ρ									TRUE	FALSE	TRUE	TRUE
ρ_1										TRUE	TRUE	TRUE
ρ_2											TRUE	TRUE
ω												TRUE
ω_1												

References

[1] R.K. Rai, M. Nepal, B.S. Karky, N. Timalsina, M.S. Khadayat, N. Bhattarai, Opportunity costs of forest conservation in Nepal, Front. For. Glob. Change 5 (2022) 1–9.

[2] J.R. Kideghesho, Realities on deforestation in Tanzania: trends, drivers, implications and the way forward, in: M. Zlatic (Ed.), Precious Forests, 1st edition, IntechOpen, Rijeka, Crotia, 2015, pp. 21–47, Ch. 2.

[3] P.A. López-Bedoya, M. Bohada-Murillo, M.C. Ángel-Vallejo, L.D. Audino, A.V. Davis, G. Gurr, J.A. Noriega, Primary forest loss and degradation reduces biodiversity and ecosystem functioning: a global meta–analysis using dung beetles as an indicator taxon, J. Appl. Ecol. 2022 (59) (2022) 1572–1585, https://doi.org/10.1111/1365-2664.14167.

[4] FAO, UNEP, The state of the world's forests 2020: forests, biodiversity and people, Technical Report, FAO, Rome, Italy, 2020.

[5] S.M. Bwalya, Household dependence on forest income in rural Zambia, Zamb. Soc. Sci. J. 2 (1) (2013) 67–86.

[6] M.A. Pratama, R.N. Zikkah, N. Anggriani, A.K. Supriatna, A mathematical model to study the effects of population pressure on two-patch forest resources, in: AIP Conference Proceedings, vol. 2264, AIP Publishing LLC, 2020, pp. 1–9.

[7] K. Lata, A.K. Misra, J.B. Shukla, Modeling the effect of deforestation caused by human population pressure on wildlife species, Nonlinear Anal., Model. Control 23 (3) (2018) 303–320, https://doi.org/10.15388/NA.2018.3.2.

[8] K. Lata, A.K. Misra, Modeling the effect of economic efforts to control population pressure and conserve forestry resources, Nonlinear Anal., Model. Control 22 (4) (2017) 473–488, https://doi.org/10.15388/NA.2017.4.4.

[9] W. Wu, Y. Li, Y. Hu, Y. Chang, Z. Xiong, Anthropogenic effect on forest landscape pattern and Cervidae habitats in northeastern China, J. Geogr. Sci. 29 (7) (2019) 1098–1112.

[10] M. Agarwal, R. Pathak, Conservation of forestry biomass and wildlife population: a mathematical model, Asian J. Math. Comput. Res. 4 (1) (2015) 1–15.

[11] A.K. Misra, K. Lata, A mathematical model to achieve sustainable forest management, Int. J. Model. Simul. Sci. Comput. 6 (4) (2015) 1–18, https://doi.org/10.1142/S1793962315500403.

[12] B. Dubey, S. Sharma, P. Sinha, J.B. Shukla, Modelling the depletion of forestry resources by population and population pressure augmented industrialization, Appl. Math. Model. 33 (7) (2009) 3002–3014, https://doi.org/10.1016/j.apm.2008.10.028.
[13] K. Jyotsna, A. Tandon, A mathematical model studying the survival of forest resource–dependent wildlife population in the presence of population pressure–induced mining activities, Nat. Resour. Model. 30 (4) (2017) 1–25, https://doi.org/10.1111/nrm.12139.
[14] I.M. Fanuel, D. Kajunguri, F. Moyo, Modelling the impact of human population and its associated pressure on forest biomass and forest-dependent wildlife population, J. Appl. Math. 2023 (2023) 4826313, https://doi.org/10.1155/2023/4826313.
[15] S. Marino, I.B. Hogue, C.J. Ray, D.E. Kirschner, A methodology for performing global uncertainty and sensitivity analysis in systems biology, J. Theor. Biol. 254 (1) (2008) 178–196.
[16] A.Z. Dragicevic, The economics of the sylvo-cynegetic equilibrium, For. Policy Econ. 120 (2020) 102300.
[17] M. Renardy, C. Hult, S. Evans, J.J. Linderman, D.E. Kirschner, Global sensitivity analysis of biological multiscale models, Curr. Opin. Biomed. Eng. 11 (2019) 109–116.
[18] J.B. Shukla, R. Pathak, M. Agarwal, Y. Takeuchi, Modeling the depletion of forest resources by population and industrialization and their conservation by green belts plantation, Int. J. Math. Model. Anal. Complex Syst., Nat. Soc. 3 (1) (2017) 7–36.
[19] A.K. Misra, A. Jha, Modeling the effect of population pressure on the dynamics of carbon dioxide gas, J. Appl. Math. Comput. 67 (1) (2021) 623–640, https://doi.org/10.1007/s12190-020-01492-8.
[20] R. Pathak, V. Verma, M. Agarwal, Impact of human activities on forest resources and wildlife population, Comput. Ecol. Softw. 11 (2) (2021) 83–99.
[21] M.D. Goshu, M.F. Endalew, Mathematical modeling on conservation of depleted forestry resources, Nat. Resour. Model. 35 (2022) 1–21.
[22] Y. Yang, H. Li, L. Cheng, Y. Ning, Effect of land property rights on forest resources in southern China, Land 10 (4) (2021) 1–15.
[23] C. Mersmann, Links between trade and sustainable forest management: an overview, Unasylva 55 (219) (2004) 3–9.
[24] D. Heine, E. Hayde, M.G. Faure, Letting commodity tax rates vary with the sustainability of production, in: Designing Fiscal Instruments for Sustainable Forests, The World Bank, Washington, DC, USA, 2021, pp. 145–171.
[25] B. Surya, S. Syafri, H. Sahban, H.H. Sakti, Natural resource conservation based on community economic empowerment: perspectives on watershed management and slum settlements in Makassar City, South Sulawesi, Indonesia, Land 9 (4) (2020) 104.
[26] D.C. Marvin, L.P. Koh, A.J. Lynam, S. Wich, A.B. Davies, R. Krishnamurthy, E. Stokes, R. Starkey, G.P. Asner, Integrating technologies for scalable ecology and conservation, Glob. Ecol. Conserv. 7 (2016) (2016) 262–275, https://doi.org/10.1016/j.gecco.2016.07.002.
[27] R.M. Sibly, J. Hone, Population growth rate and its determinants: an overview, Philos. Trans. R. Soc. Lond. B, Biol. Sci. 357 (1425) (2002) 1153–1170.
[28] B. Gomero, Latin hypercube sampling and partial rank correlation coefficient analysis applied to an optimal control problem, Master' thesis, University of Tennessee, 2012.
[29] S.M. Blower, H. Dowlatabadi, Sensitivity and uncertainty analysis of complex models of disease transmission: an HIV model, as an example, Int. Stat. Rev. (Rev. Int. Stat.) 62 (2) (1994) 229–243.
[30] S.A. Pedro, H. Rwezaura, J.M. Tchuenche, Time–varying sensitivity analysis of an influenza model with interventions, Int. J. Biomath. 15 (3) (2022) 1–27.
[31] H. Bauer, G. Chapron, K. Nowell, P. Henschel, P. Funston, L.T. Hunter, D.W. Macdonald, C. Packer, Lion (Panthera leo) populations are declining rapidly across Africa, except in intensively managed areas, Proc. Natl. Acad. Sci. 112 (48) (2015) 14894–14899.
[32] M.Y. Li, An Introduction to Mathematical Modeling of Infectious Diseases, vol. 2, Springer, Washington, DC, USA, 2018.
[33] I.J. Myung, Tutorial on maximum likelihood estimation, J. Math. Psychol. 47 (1) (2003) 90–100, https://doi.org/10.1016/S0022-2496(02)00028-7.
[34] J.C. Lagarias, J.A. Reeds, M.H. Wright, P.E. Wright, Convergence properties of the Nelder–Mead simplex method in low dimensions, SIAM J. Optim. 9 (1) (1998) 112–147.
[35] A. Saltelli, Sensitivity analysis: could better methods be used?, J. Geophys. Res., Atmos. 104 (D3) (1999) 3789–3793.
[36] Y. Dai, J.L. Stanford, M. LeBlanc, A multiple-testing procedure for high-dimensional mediation hypotheses, J. Am. Stat. Assoc. 117 (537) (2022) 198–213.
[37] A.K. Misra, K. Lata, J.B. Shukla, Effects of population and population pressure on forest resources and their conservation: a modeling study, Environ. Dev. Sustain. 16 (2) (2014) 361–374.
[38] A.K. Misra, K. Lata, Depletion and conservation of forestry resources: a mathematical model, Differ. Equ. Dyn. Syst. 23 (1) (2013) 25–41, https://doi.org/10.1007/s12591-013-0177-3.